1/f BASEBAND NOISE SUPPRESSION IN OFDM USING KALMAN FILTER

T.Prem kumar[#1], P.Viswanath[=2],S.Sai Sandeep[#3]

[#1,2]Assistant Professor, Electronics and Communication Engineering, SACET, JNTU Kakinada Chirala, Andhra Pradesh, India

[#1]premtagore@gmail.com

[#2]viswanathponugoti@gmail.com

[#3]Assistant Professor, Electronics and Communication Engineering, SACET, JNTU Kakinada Chirala, Andhra Pradesh, India

[#3]saisiddhu.99@gmail.com

1.Abstract:

The commonly used direct-conversion Radio Frequency (RF) chips exhibit an additive 1/f baseband noise around the DC. The 1/f noise level increases as the transistors inside the RF chip become ever smaller. This type of noise mainly affects the low frequencies and can be very significant for small frequency allocations around the DC in Orthogonal Frequency-Division Multiple Access (OFDMA) systems. In this article we present the effects of such 1/f baseband noise on small frequency allocations for a Long Term Evolution (LTE) User Equipment (UE). We proceed to estimate the 1/f baseband noise. Suppression of the 1/f baseband noise is achieved by subtracting the estimated 1/f baseband noise from the received signal. We show that considerable processing gain is achieved when the 1/f baseband noise suppression is applied.

Index Terms—1/f noise, OFDM, direct conversion, baseband noise.

2.INTRODUCTION

As Very-Large-Scale Integration (VLSI) technology advances, the transistors inside chips become consistently smaller. One harmful effect of this down-sizing is the evolution of stronger $1/f$ noise. As the feature size of Metal Oxide Semiconductor (MOS) devices is scaled to achieve higher speed and greater packing density, the flicker noise, or $1/f$ noise, spectra increases as $1/L^3_{g(min)}$ where $L_{g(min)}$ is the minimum gate length [1, and references therein]. This $1/f$ noise is additive by nature. Due to the $1/f$ noise spectral shaping, it mainly impairs frequencies around the DC. Such $1/f$ noise is common in baseband Analog Front Ends (AFE) utilizing Direct-Conversion RF (DCR) [2], used by many communication systems such as OFDMA transceivers. In [3], the effects of $1/f$ noise in the transmitter were considered for OFDM systems by evaluating the Error Vector Magnitude (EVM). For a wide-band system, impairment of a small subset of frequencies around the DC may be insignificant. However, in OFDMA systems, the frequency allocation to a specific user might be a small one around the DC. Such a frequency allocation would be seriously affected by the $1/f$ noise. In fact, in the 3GPP Long Term Evolution specification (LTE) [4] the basic allocation unit, termed Resource Block (RB), consists of twelve subcarriers. The subcarrier spacing in LTE is $15KHz$, thus one RB has $180KHz$ bandwidth. A User Equipment (UE) may be allocated a single RB near the DC, and thus it is important to study the effects of the $1/f$ baseband noise on overall performance. One way to mitigate the effects of the baseband $1/f$ noise would be to pre-compensate at the TX with a small power increase around DC. However, as each receiver is likely to have a different level of $1/f$ noise that depends on implementation and also on external parameters such as temperature, the base-station TX will have to be notified by each receiver of this value. This will place an excessive load on the UE uplink. Furthermore, this will only be applicable in case the Channel State Information (CSI) is perfectly known, which is not commonly the case; especially at high speeds. In this paper we investigate the effects of $1/f$ baseband noise on a small frequency allocation for an LTE UE. We further utilize the $1/f$ noise model in [5] to estimate the $1/f$ noise. We show that suppression of the $1/f$ noise by subtracting the

estimated $1/f$ noise from the received signal, results in a significant processing gain. The estimation of the $1/f$ noise is done by the well-known Kalman filter [6], which computes a new estimate for every received sample. This type of processing is appropriate for real-time systems such as an LTE UE transceiver. The UE transceiver will be most vulnerable to the $1/f$ baseband noise while receiving a very weak signal while operating in sensitivity, which is defined as the minimum signal received from the antenna connector [7]. The reception at sensitivity is a very important parameter in a cellular system, since it determines the transceiver's capability of operating at the cell edge. This in turn, determines the possible spatial separation of the costly base stations, termed evolved Node B (eNB) in LTE. In section 3 we define the system model. In section 4 we present a scheme for estimating the $1/f$ baseband noise using a Kalman filter. In section 5, an applicative example is given for an LTE UE transceiver. We explore the damages of the $1/f$ baseband noise on small frequency allocations around the DC. We suppress the $1/f$ noise by subtracting the $1/f$ noise estimation from the received signal. The suppression of the $1/f$ noise results in considerable processing gain. Concluding remarks are given in section 6.

3.SYSTEM MODEL

In [5] a $1/f$ noise model is developed that consists of N +1first-order differential equations, where N is a model parameter determining the accuracy of the $1/f$ model. The $1/f$ noise model is given by

$$\dot{y}_{2N}(t) = y_{2N}(t) - y_{2N}(0) + 2\left[v(t) - \emptyset(t) - 2\sum_{k=1}^{N} y_{2k}(t)\right]$$

$$\dot{y}_{2N-2(t)} = y_{2N-2}(t) - y_{2N-2}(0) - 4y_{2N}(t) + 4\left[v(t) - \emptyset(t) - 2\sum_{k=1}^{N} y_{2k}(t)\right]$$

$$\dot{y}_{2N-4}(t) = y_{2N-4}(t) - y_{2N-4}(0) - 4y_{2N}(t) - 8y_{2N-2}(t) - 6\left[v(t) - \emptyset(t) - 2\sum_{k=1}^{N} y_{2k}(t)\right]$$

$$\vdots$$

$$\begin{aligned}
\dot{y}_2(t) &= y_2(t) - y_2(0) - 4\sum_{m=1}^{N-1} m y_{2(N-m+1)}(t) + \\
&\quad 2N\left[\nu(t) - \phi_n(t) - 2y_2(t)\right] \\
\dot{\phi}(t) &= -(2N+1)\phi(t) - \phi(0) - \\
&\quad 4\sum_{m=1}^{N} m y_{2(N-m+1)}(t) + 2(N+1)\nu(t), \quad (1)
\end{aligned}$$

where $\nu(t)$ is a white Gaussian noise process with unit spectral density and $\phi(t)$ is the approximated $1/f$ Gaussian process. Thus, the N^{th} approximation to the $1/f$ noise process is an output of a Markovian system of N+1 linear stochastic differential equations of Itô type [8]. The equations in (1) can also be written in vector form

$$\dot{x}(t) = Fx(t) + Gv(t) \quad (2)$$

where the matrices $\boldsymbol{F}$ and $\boldsymbol{G}$ are given by

$$F = \begin{bmatrix} -3 & -4 & -4 & \cdots & -4 & -2 \\ -4 & -7 & -8 & \cdots & -8 & -4 \\ -4 & -8 & -11 & \cdots & -12 & -6 \\ \vdots & \vdots & \vdots & \ddots & \vdots & \vdots \\ -4 & -8 & -12 & \cdots & -4N-1 & -2N \\ -4 & -8 & -12 & \cdots & -4N & -2N-1 \end{bmatrix} \quad (3)$$

and

$$G = \begin{bmatrix} 2 \\ 4 \\ \vdots \\ 2N \\ 2(N+1) \end{bmatrix} \quad (4)$$

respectively and the state vector $\boldsymbol{x}(t)$ is defined as

$$x(t) = \begin{bmatrix} y_{2N}(t) \\ y_{2N-2}(t) \\ \vdots \\ y_2(t) \\ \emptyset(t) \end{bmatrix} \quad (5)$$

The dimensions of $\boldsymbol{F}$, $\boldsymbol{G}$ and $\boldsymbol{x}$ are $(N+1)\times(N+1)$, $(N+1)\times 1$ and $(N+1)\times 1$ respectively. The model for the $1/f$ noise in (2) is for continuous time whereas a discrete time model is needed. The solution to (2) can be derived by integration. Such integration can be achieved by using Van Loan's [9] work that employs a diagonal Padé approximation with scaling and squaring. Kasdin [10] employed Van Loan's work to derive a discrete time model from a continuous one. We shall use the formalism in [10] to develop a discrete time model for (2). Following the notation in [10, Appendix I], let us define

$$C = \begin{bmatrix} -F & QG^T \\ 0 & F^T \end{bmatrix} \quad (6)$$

where $\boldsymbol{F}$ and $\boldsymbol{G}$ are defined in (3) and (4) respectively. The parameter Q is used to control the intensity of the $1/f$ noise. The dimensions of the matrix $\boldsymbol{C}$ are $(2N+2)\times(2N+2)$. Next let us define the matrix

$$e^{C_{\Delta t}} = \begin{bmatrix} F_2 & G_2 \\ 0 & F_3 \end{bmatrix} \quad (7)$$

where Δt is the desired time span between two samples of the discrete process. The dimensions of the matrices $\boldsymbol{F}_2$, $\boldsymbol{G}_2$ and $\boldsymbol{F}_3$ are $(N+1)\times(N+1)$. Now using (3) and (7), we shall define

$$\begin{aligned} Q_d &= F_3{}^T G_2 \\ \Phi &= e^{F\Delta_t} \end{aligned} \quad (8)$$

both having dimension $(N+1)\times(N+1)$. Using (8) the discrete model is given as [10, eq. 53]

$$\boldsymbol{\xi}_{k+1} = \Phi\boldsymbol{\xi}_k + \boldsymbol{w_k} \quad (9)$$

where $\boldsymbol{w_k}$ is an Independent and Identically-Distributed (IID) Gaussian vector process with covariance matrix $\boldsymbol{Q_d}$. The last element of $\boldsymbol{\xi}_k$ is the desired $1/f$ sampled process and shall be denoted by ϕ_k. The$1/f$ noise level is determined by the parameter Q in (6), with spectral density

$$S_{\phi\phi}(f) = \frac{Q}{2\pi|f|} \quad (10)$$

During a symbol time T, the complex envelope of the transmitted OFDM signal can be expressed as [11]

$$s(t) = \left(h(t) \otimes \sum a_m e^{j2\pi\frac{m}{T}t}\right). \quad (11)$$

The data am modulates the sinusoid at frequency m/T during the OFDM symbol time T. The channel impulse response is denoted by $h(t)$. Usually, a few samples from the end of a symbol are copied and inserted at the beginning of the symbol. The samples inserted at the beginning of the symbol are termed Cyclic Prefix (CP), and are used to avoid Inter Symbol Interference (ISI) due to the time dispersiveness of the channel $h(t)$. The received complex signal rk at the transceiver's baseband, after sampling at the appropriate rate, may be written as

$$r_k = s_k + v_k + \phi_{I,k} + j\phi_{Q,k} \quad (12)$$

WHERE v_k IS A CIRCULAR COMPLEX ADDITIVE IID GAUSSIAN THERMAL NOISE PROCESS AND BOTH $\phi_{I,k}$, $\phi_{Q,k}$ HAVE SPECTRAL DENSITY (10). THE THERMAL NOISE v_k VARIANCE IS DEFINED SUCH THAT IT HAS N_0 VARIANCE FOR EVERY SUBCARRIER IN THE FREQUENCY DOMAIN

4.BASEBAND $1/f$ NOISE ESTIMATION SCHEME

The s_k component in (12) can be viewed as noise for the sake of estimating the $1/f$ noises $\phi_{I,k}$ and $\phi_{Q,k}$. In fact, since the OFDMA signal is composed of randomly phased symbols in the frequency domain, the resulting time domain samples after Inverse Fast Fourier Transform (IFFT) have Gaussian noise like behaviour. Using the discrete-time $1/f$ model (9), the well-known Kalman filter [6] is applied to estimate the noise processes $\phi_{I,k}$ and $\phi_{Q,k}$. The observation is given in (12) where $s_k + v_k$ is the observation noise. The estimation of $\phi_{I,k}$ shall be done on the real part of r_k, whereas the estimation of $\phi_{Q,k}$ shall be done on the imaginary part of r_k. In the sequel, the notation $\hat{}\,\phi_{k|\ k}$ shall be used to denote the separate estimation of the real and the imaginary parts of the baseband $1/f$ noise. When the observation $\tilde{r}_k$ in (16) equals the real part of r_k, then $\hat{\phi}_{k|k}$ is the estimate of $\phi_{I,k}$, and when $\tilde{r}_k$ equals the imaginary part of r_k, then $\hat{\phi}_{k|k}$ is the estimate of $\phi_{Q,k}$. The estimation of $\hat{\phi}_{k|k} = \boldsymbol{H}\hat{\boldsymbol{\xi}}_{k|k}$ shall be recursively computed using the Kalman filter, where H is given by

$$\boldsymbol{H^T} = \begin{bmatrix} 0 \\ 0 \\ \vdots \\ 0 \\ 1 \end{bmatrix}. \quad (13)$$

The first step is the prediction stage

$$\hat{\xi}_{k|k-1} = F\hat{\xi}_{k-1|k-1} \quad (14)$$

$$P_{k|k-1} = FP_{k-1|k-1}F^T + Q_d \quad (15)$$

where the a-priori predicted estimate state $\hat{}\,\xi k|k-1$ is given by(14) and the a-priori predicted estimate covariance

TABLE I
SIMULATION PARAMETERS

Parameter	*Unit*	*Value*
TTI	ms	1
Symbols in Slot		7
Slots in Sub-frame		2
Bandwidth	MHz	10
FFT size		1024
Guard tones per symbol		424
Number of usable tones		600
Number of layers		1
Coding Rate		0.21
Modulation		QPSK
MCS		5
Number of RBs per OFDM symbol		50
Reference signal boosting	dB	0

$P_{k|k-1}$ is given by (15). The second step is the update stage

$$\bar{r}_k = \tilde{r}_k - H\hat{\xi}_{k|k-1} \quad (16)$$

$$S_k = HP_{k|k-1}H^T + R \quad (17)$$

$$K_k = P_{k|k-1}H^T S_k^{-1} \quad (18)$$

$$\hat{\xi}_{k|k} = \hat{\xi}_{k|k-1} + K_k\bar{r}_k \quad (19)$$

$$P_{k|k} = (I - K_k H)P_{k|k-1} \quad (20)$$

where the observation $\tilde{r}_k$ in (16) is either the real or imaginary part of the k[th] sample entering the receiver, R in (17) is the variance of $s_k + v_k$ in (12), $\bar{r}_k$ is the innovation (16), S_k is the innovation covariance (17), K_k is the optimal Kalman gain (18), $\hat{\xi}_{k|k}$ is the updated state estimate (19) and $P_{k|k}$ is the updated estimate covariance (20).

We define the initial conditions as

$$\hat{\xi}_{0|0} = 0, P_{0|0} = Q_d. \quad (21)$$

The variance R in (17) needs to be estimated from the received samples. One option is to estimate the power of the received samples at the output of a high-pass filter with a low frequency cut off at the $1/f$ noise corner frequency [3]. Another option is to estimate R by subtracting the estimated $1/f$ noise power from the total power of the received samples. This method was adopted for the simulations results presented in this paper. The power level Q of the $1/f$ noise, and subsequently the matrix Q_d, can be determined at RF calibration. The $1/f$ power level Q is due to the physics of the implementation and will change slowly as a function of external parameters such as temperature. These changes can be tracked by periodic RF calibrations or by using the output of the proposed estimation scheme. In fact, by tracking the changes of the $1/f$ noise level using the output of the estimation, one can indirectly monitor changes in external parameters such as temperature changes. The reliability of the $1/f$ estimation can be determined through the (N +1,+1)element of $P_{k|k}$ (20), which is the estimated error variance of the estimation. It is important to note that many elements in the estimation process are scalar values, and most importantly S_k in (17) is a scalar and thus the matrix inversion in (18) is replaced by simple scalar division. In the low SNR (see 24) scenarios, the estimation of the $1/f$ noise and consequently its suppression, result in a substantial processing gain. The stronger the $1/f$ noise, the higher the expected processing gain that results from the $1/f$ noise suppression since the noise, that is actually the desired signal plus additive thermal noise, remains constant.

A. 5. LTE UE TRANSCEIVER-AN APPLICATIVE EXAMPLE

B. *To demonstrate both the effect of the $1/f$ baseband noise and the effect of its suppression, the LTE cellular specification is given as an applicative example. A 10MHz bandwidth LTE eNB signal is simulated passing through an EVA channel $h(t)$ [12, Appendix B.2], between the transmit (TX) antenna and receive (RX) antennas. The handset speed relative to the eNB is 38Kmph, which translates to 70Hz Doppler spread for carrier frequency of 2GHz. The eNB is configured with one TX antenna and the UE is configured with two RX antennas. The receiver implements a Maximal Ratio Combining (MRC) decoder [4] to detect the incoming signal in the frequency domain, after the usual Cyclic Prefix (CP) removal and the transition to the frequency domain by the application of a Fast Fourier Transform (FFT). Perfect timing and frequency estimation is assumed. A frequency domain Linear Minimum Mean Square Error (LMMSE) Channel Estimator (CE) using the nearest five Reference Signals (RS) is applied for every data subcarrier. Other simulation parameters are given in table I. The additive $1/f$ baseband noise in the simulation is generated by using (9) with model order of N = 100. Note that later, the estimation of the $1/f$ noise by Kalman filter shall use (9) with a model order of N=5 to simplify the receiver implementation. Furthermore, the $1/f$ baseband noise is also generated by an independent exact model [10]. By generating the $1/f$ noise using an independent model, it is demonstrated that the estimation of the $1/f$ noise is not tailored solely to the model developed in this work. It is important to note that the estimation of the $1/f$ noise in the receiver using the Kalman filter is still based on the model in (9), regardless of the way the $1/f$ baseband noise was actually generated. For completeness the $1/f$ noise model in [10] is reproduced below***

C.

$$\emptyset_n = \sum_{k=1}^{n} -a_k \emptyset_{n-k} + u_n \quad (22)$$

D. *where the coefficients a_k are given by*

E.

$$a_0 = 1, a_k = (k - 1 - \frac{1}{2})\frac{a_k - 1}{k} \quad (23)$$

F. *and un is an IID Gaussian random variable with variance Q. Although this model is useful for generation purposes, it does not allow direct application of a Kalman filter for estimation. The run time for the exact model is significantly longer than the run time for the approximated $1/f$ noise model, since in the exact $1/f$ noise model the generation of each new sample involves all of the previously generated $1/f$ noise samples. In fact, this strong dependency of each new sample on past samples is exactly the reason why the slowly changing characteristics of the $1/f$ noise can be estimated. In Fig. 1 the results for a single RB allocation near the DC are presented. A $10MHz$ LTE signal consists of fifty RBs, twenty-five on each side of the DC. The allocated RB is twenty-five, where the first RB having the lowest frequency is termed RB zero. The x-axis in Fig. 1 represent the SNR defined as*

G. $$SNR = \frac{E_s}{N_0}$$

H. *where Es is the subcarrier mean energy, and N_0 is the white thermal baseband noise energy for a single subcarrier. In Fig. 1 four types of curves are shown: the BLock Error Rate (BLER) when the $1/f$ baseband noise is not present, the BLER in the presence of the $1/f$ complex baseband noise and the BLER in the presence of the$1/f$ complex baseband noise, generated both by using the model (9) and by using the exact model (22), after suppression of the $1/f$ complex baseband noise. The $1/f$ noise estimation was done using the model in (9) with model order of N =5. This means that the matrices in (14)-(20) F, $P_{k|k-1}$, $P_{k-1|k-1}$ and Q_d are of dimension 6×6 and that the vectors $\xi_{k|k-1}$, $\xi_{k-1|k-1}$, H and K_k are of dimension 6×1. The$1/f$ noise strength is defined using Q (10). The $1/f$ noise strength is sometimes defined by a corner frequency which corresponds to the frequency where the $1/f$ noise spectral density equals the system noise floor. Bipolar devices typically have corners of tens or hundreds of Hz, whereas MOS devices have corners of tens of KHz to a few MHz [3]. Let us assume SNR level of $0dB$ for example. Since $0dB$ SNR means that the noise power is equal to the signal power inside one $15KHz$ subcarrier, the thermal noise power spectral density is 1/15000 assuming Es =1. A corner frequency of $1MHz$ means*

I. $$\frac{Q}{2\pi 10^6} = \frac{1}{15 \times 10^3} \qquad (25)$$

J. *Thus, for a $1MHz$ corner frequency we get Q=26.2dB.For simulation and understanding purposes it is convenient to normalize Es to one when SNR =0dB. In real applications the thermal noise and $1/f$ noise are determined by the physics of the implementation, and changes in Es cause the changes in the SNR. Multiplying the triplet signal level, thermal noise level and $1/f$ noise level by a constant does not change the performance. In Fig. 1, Q is defined to be in the range of $19-23dB$ (cut off frequency between $190KHz$ and $476KHz$ respectively).*

K. 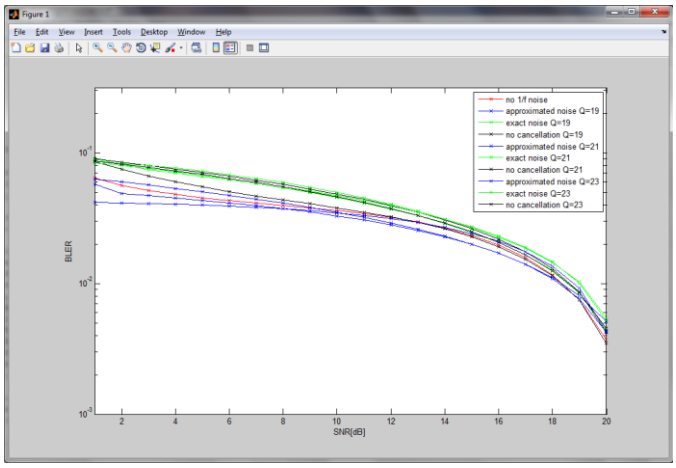

L. ***Fig. 1. BLER for single RB allocation near the DC.Solid curves denote the normalized throughput when suppression of $1/f$ noise is applied, the generation of the noise is done using an approximated $1/f$ with N = 100 for lines with circles and using an exact model for lines with pluses. Dashed curves denote the BLER when no suppression of $1/f$ noise is applied. For reference, the BLER when no $1/f$ noise is present is denoted by a dash-dot curve. Q is defined to be $19dB$, $21dB$, and$23dB$ that correspond to a cut off frequency of $190KHz$, $300KHz$, and$476KHz$ respectively. All results are based on the simulation of 100 frames***

M. *A significant gain can be seen for BLER smaller than 0.3. Common practice is to target a UE to work in a setting where the BLER is between 0.1 and 0.3. For higher BLER levels, we can expect a lower MCS. It can be seen that the degradation of performance rises quickly for small increments of the $1/f$ baseband noise level. In general, this relaxation in $1/f$ noise tolerance may be translated to a simpler AFE design and to lower power consumption. It can also be seen that the results are almost exactly the same whether the $1/f$ noise was generated by the approximated model or whether it was generated by the exact model. To get a better picture of the estimation process of the $1/f$ baseband noise, in Fig. 2 the real part of the received sampled signal r_k, the real part of the $1/f$ baseband noise and the estimation of the real part of the $1/f$ baseband noise are presented. In Fig. 2 it can be seen that the estimation of the $1/f$ noise follows the low frequency variations of the $1/f$ noise. Considering $s_k + v_k$ to be the desired signal,*

N. *the Normalized Mean Square Error ($NMSE$) before the $1/f$ noise suppression is defined*

O. $$NMSE_{before} = 10log_{10}\frac{\sum|\phi_{I,k} + j\phi_{Q,k}|^2}{\sum|s_k + v_k|^2}. \qquad (26)$$

P. ***For example, the NMSE is calculated for $Q = 24dB$ before the $1/f$ noise suppression to be $-4.8dB$. In a similar fashion the NMSE after the $1/f$ noise suppression is defined***

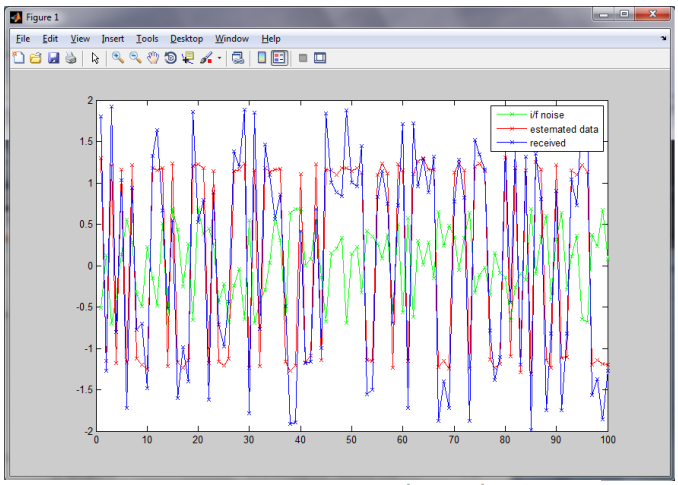

Q.

$$NMSE_{after} = 10log_{10}\frac{\sum|\phi_{I,k} + j\phi_{Q,k} - \hat{\phi}_{I,k} - j\hat{\phi}_{Q,k}|^2}{\sum|s_k + v_k|^2}. \quad (27)$$

R. ***For the same data, the NMSE after the $1/f$ noise suppression resulted as $-6.7dB$. In case of perfect cancelation, the NMSE is $-\infty$ .As the sum of signal strength and thermal noise decreases or as the $1/f$ noise strength increases,***

S. ***Fig. 2. Time domain phase noise estimation: the blue signal is the received signal, the green signal is the $1/f$ noise, and the red signal is the estimation of the $1/f$ noise from the received signal.***

T. ***the potential gain and the achieved gain increase. Since the approximation of the $1/f$ noise turns out as a linear system of first-order stochastic differential equations driven by white Gaussian noise, the Kalman filter gives the best estimator having the minimal Mean Square Error (MSE) and thus the minimal achievable NMSE after noise cancellation. A consistent allocation of one RB adjacent to the DC is unlikely for systems with a high bandwidth. However, studying the effects of this type of allocation is important since it concentrates on the impairment of the $1/f$ baseband noise. This type of allocation will occur more frequently in a $1.4MHz$ LTE system where there are only six RBs, two of which are adjacent to the DC.***

U. ***For high MCS with a wide- band allocation, the impairment of a single RB can have severe implications. As the size of the frequency allocation grows bigger, the dependency on the subcarriers near the DC, affected by the $1/f$ baseband noise, will become smaller. However, even for large frequency allocations, the suppression of the $1/f$ baseband noise can become helpful for high enough coding rates where the redundancy is small enough such that each subcarrier counts. In Fig. 3 results are shown for a six RB allocation around the DC, which constitutes the maximal frequency allocation for a $1.4MHz$ LTE system. In the figure, the BLER is given as a function of Q for constant $Es/N0 = 6dB$. The channel used for the simulation was EVA with UE speed of $38Kmph$. It can be clearly seen that the $1/f$ baseband noise suppression is useful for larger allocations than one RB adjacent to the DC. Another insightful representation of the gains that result from the $1/f$ baseband noise suppression, is to graph the processing gain in the y-axis vs. the remaining $1/f$ noise level after suppression in the x-axis. The remaining $1/f$ noise level after suppression is given as the ratio between the residual level of $1/f$ noise after suppression and between the $1/f$ noise level before suppression. Note that the remaining $1/f$ noise level after suppression is a value between zero and one. In Fig. 4, such curves are provided for $1/f$ baseband noise levels of $Q = 19dB$, $Q = 21dB$ and $Q = 23dB$ (corresponding***

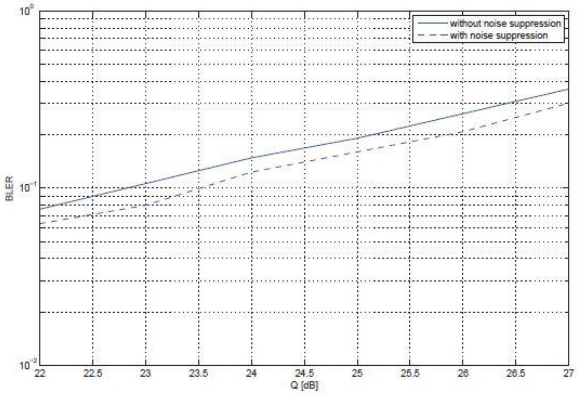

Fig. 3.BLER for six RB allocation around the DC. Solid curve denotes the BLER when suppression of $1/f$ noise is not applied. Dashed curve denote the BLER when suppression of $1/f$ noise is applied. All results are based on the simulation of 100 frames. The channel was EVA with UE speed

of $38Kmph$. The SNR E_s/N_0 was set at a constant $6dB$. Q is defined to be in the range of $22-27dB$ (cut off frequency between $378KHz$ and $1.2MHz$ respectively).

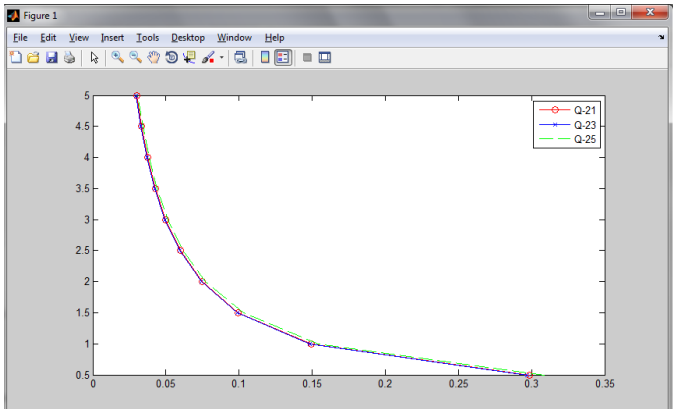

Fig. 4. Processing gain vs. the remaining 1/f noise level after suppression. Curves are given for 1/f noise level Q of 19dB, 21dB, and23dB that correspond to a cut off frequency of 190KHz, 300KHz, and476KHz respectively

to cut off frequencies of 300KHz, 476KHz and 755KHz correspondingly). For the same level of normalized remaining baseband noise, the processing gain is higher when the value of Q is higher. This is because the total level of noise suppressed when Q is higher is larger for the same normalized remaining noise level. In all previous examples a noise model of approximation order N=5was used for the estimation. The approximation order greatly affects the complexity of the suggested scheme. To determine what approximation order is required for good noise suppression, we simulated a six RB allocation around the DC with constant Q = 19dB and different approximation orders ranging from one to six. The channel used for the simulation was EVA with UE speed of 38Kmph. The results are given in Fig. 5. It can be seen that an approximation order of N=5 is enough in order to

V. *achieve good results.*

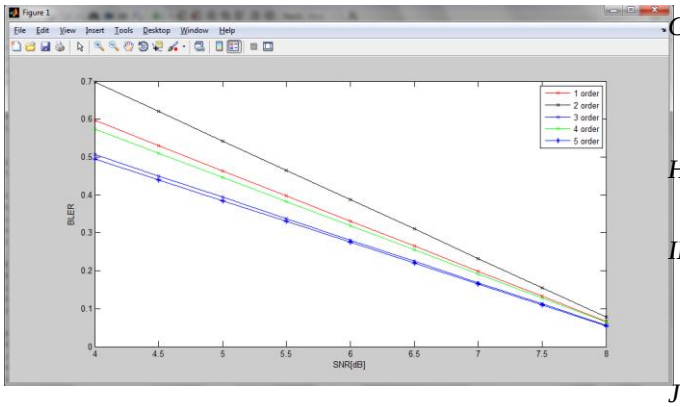

W.

X. *Fig. 5. BLER for single RB allocation near the DC. The 1/f noise level was set at Q = 19dB (cutoff frequency of 190KHz). Approximation order N used for the estimation of the 1/f noise was set to values ranging from one to six.*

Y. *The estimation of the 1/f noise is applied to each new sample at the receiver input. However, almost all the 1/f noise power resides inside the corner frequency of the noise. Therefore the estimation can be performed on the received data after passing through a low-pass filter with a cut off frequency set at the corner frequency. The data after low-pass filtering can be down sampled at the appropriate rate to save computations.*

Z. *6. CONCLUSION*

AA. *As VLSI technology utilizes ever smaller transistors, the effects of 1/f noise become increasingly dominant. This 1/f noise is particularly significant for DCR architectures with MOS technology. The effects of the 1/f baseband noise on small frequency allocations near the DC were investigated, using the LTE UE as an applicative example. A scheme for the suppression of the 1/f noise was suggested. Finally, it was shown that application of the 1/f noise suppression scheme results in significant processing gains that can be utilized to simplify the design and implementation of the AFE.*

BB. *REFERENCES*

CC. *[1] K. W. Chew, K. S. Yeo, and S.-F. Chu, "Impact of technology scaling on the 1/f noise of thin and thick gate oxide deep submicron NMOS transistors," IEE Proc. Circuits Devices Syst., no. 5, pp. 415-421, Oct. 2004.*

DD. *[2] W. Namgoong and T. H. Meng, "Direct-conversion RF receiver design," IEEE Trans. Commun., vol. 49, no. 3, pp. 518-529, Mar. 2001.*

EE. *[3] A. Georgiadis, "AC-coupling and 1/f noise effects on baseband OFDM signals," IEEE Trans. Commun., vol. 54, no. 10, pp. 1806-1814, Oct. 2006.*

FF. *[4] S. Sesia, I. Toufik, and M. Baker, LTE - The UMTS Long Term Evolution - From Theory to Practice. John Wiley & Sons, 2009.*

GG. *[5] S. Landis, Z. Schuss, and B. Z. Bobrovsky, "The exit problem in a nonlinear system driven by 1/f noise: the delay locked loop," SIAM J. Appl. Math., vol. 66, pp. 1188-1208, Apr. 2006.*

HH. *[6] A. H. Jazwinski,Stochastic Processes and Filtering Theory. Academic Press, 1970.*

II. *[7] L.-H. Li, F.-L. Lin, and H.-R. Chuang, "Complete RF-system analysis of direct conversion receiver (DCR) for 802.11a WLAN OFDM system," IEEE Trans. Veh. Technol., vol. 56, no. 4, pp. 1696-1703, July 2007.*

JJ. *[8] Z. Schuss, Theory and Applications of Stochastic Processes: An Ana- lytical Approach. Springer, 2010.*

KK. *[9] C. F. V. Loan, "Computing integrals involving the matrix exponential," IEEE Trans. Autom. Control, vol. AC-23, no. 3, pp. 395-404, June 1978.*

LL. *[10] N. J. Kasdin, "Discrete simulation of colored noise and stochastic processes and a 1/f power law noise generation," Proc. IEEE, vol. 83, pp. 802-827, May 1995.*

MM. *[11] T. Pollet, M. V. Blade, and M. Moeneclaey, "BER sensitivity of OFDM systems to carrier frequency offset and Wiener phase noise," IEEE Trans. Commun., vol. 43, no. 2/3/4, pp. 191-193, Feb./Mar./Apr. 1995.*

NN. *[12] "Evolved universal terrestrial radio access (E-UTRA); user equipment (UE) radio transmission and reception (3GPP TS 36.101 version 9.3.0 release 9)," ETSI, Technical Specification, 2010.*